Pulsar Mapping Memo #01

Sensitivity analysis of pulsar beam mapping with the LWA and VLA

Akshatha K Vydula

Sep-02-2021

Cross-correlation between VLA and LWA could be done in three modes (single LWA ant, beamformed LWA drift, beamformed LWA track). We would like a sensitivity model which allows us to predict the SNR of selected pulsars in each of these modes.

From Synthesis Radio Astronomy, we have
SEFD (source equivalent flux density) is Tsys/K

$$\Delta S_{\mathrm{ij}} = \frac{1}{\eta_{\mathrm{s}}} \sqrt{\frac{SEFD_{\mathrm{i}}\, SEFD_{\mathrm{j}}}{2\, \Delta\nu\, \tau_{\mathrm{acc}}}} \qquad (9\text{–}14)$$

Note: Lower SEFD is better

Case 1: Cross-correlation between VLA full array and LWA full array

$SEFD_{VLA}$= 5e4 Jy (from here for 70-82MHz) for a single dish

For an interferometric system with N antennas, the sensitivity can be simply calculated using:

$$Sensitivity = \frac{SEFD}{\eta_a \sqrt{N(N-1)\Delta\nu\tau_{acc}}}$$

$SEFD_{VLA}$= 5e4/ sqrt(26*(26-1)) for an array with 26 elements = 1961.16 Jy

$SEFD_{LWA}$ = 4680 Jy (from here for 75MHz)

For Tacc = 20 s and spectral bandwidth of 10MHz, noise level = 0.1514 Jy

Case 2: Cross-correlation between VLA full array and LWA single dipole

$SEFD_{VLA}$= 5e4 Jy (from here for 70-82MHz)
$SEFD_{LWA}$ = 1e6 Jy(from here for 74MHz, fig 3)

For Tacc = 100 s and spectral bandwidth of 1MHz, noise level = 2.214 Jy

Case 3: Cross-correlation between 40m LWA feed and LWA full array

$SEFD_{40m}$= 6kJy (from Danny's proposal)

$SEFD_{LWA}$ = 4680 Jy (from here for 75MHz)

For Tacc = 20 s and spectral bandwidth of 10MHz, noise level = 0.2649 Jy

Pulsars brighter than 1Jy: From ATNF Pulsar Catologue at 80MHz
Paper on the catalog:

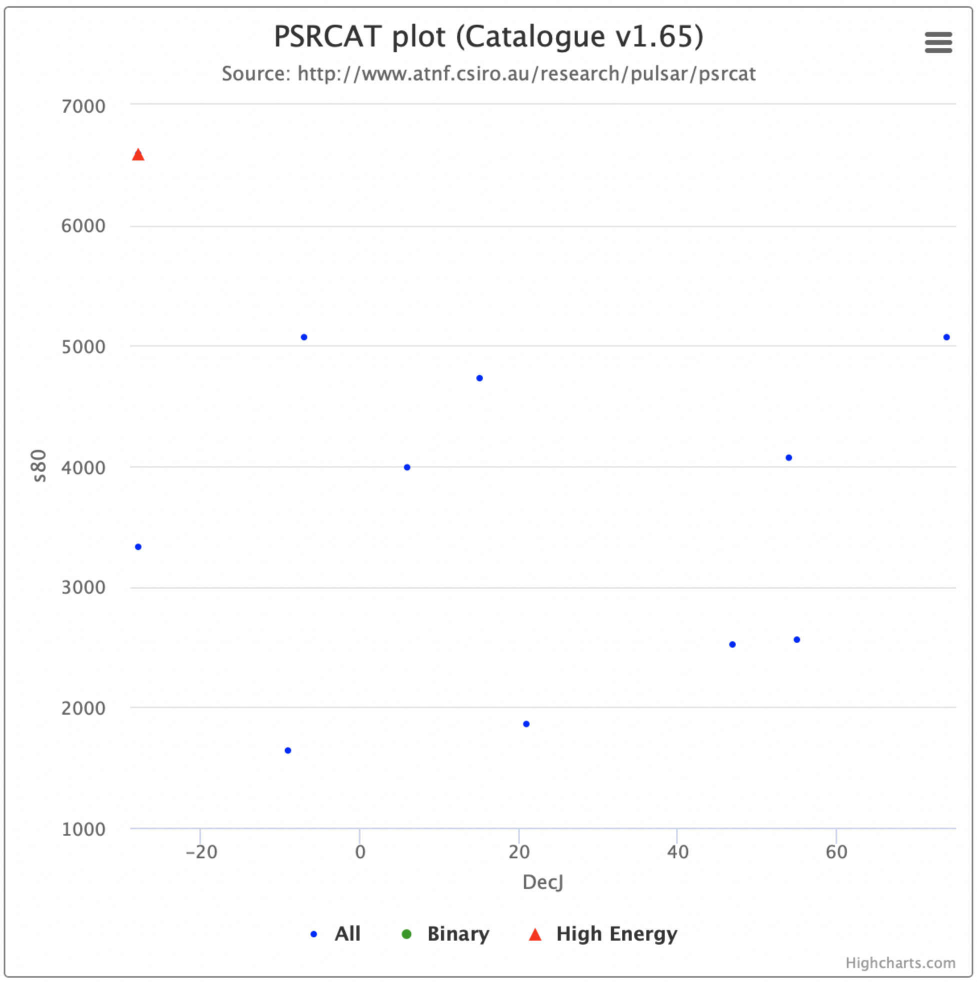

#	NAME		RAJ (hms)			DECJ (dms)			S60 (mJy)			S80 (mJy)		
1	B0628-28	lvw69a	06:30:49.404393	43	dtbr09	-28:34:42.77881	37	dtbr09	*	0	*	6590	3280	srb+15
2	B0031-07	lvw69a	00:34:08.8703	1	cbv+09	-07:21:53.409	2	cbv+09	*	0	*	5070	2540	srb+15
3	B0809+74	cp68	08:14:59.50	2	hlk+04	+74:29:05.70	11	hlk+04	*	0	*	5070	2540	srb+15
4	B1133+16	phbc68	11:36:03.1198	1	dgb+19	+15:51:14.183	1	dgb+19	*	0	*	4730	2370	srb+15
5	B0329+54	cp68	03:32:59.4096	1	dgb+19	+54:34:43.329	1	dgb+19	*	0	*	4070	2030	srb+15
6	B0834+06	phbc68	08:37:05.642	3	hlk+04	+06:10:14.56	14	hlk+04	*	0	*	3990	2000	srb+15
7	B1749-28	tv68	17:52:58.6896	17	hlk+04	-28:06:37.3	3	hlk+04	*	0	*	3330	1660	srb+15
8	B1508+55	htg+68	15:09:25.6298	1	cbv+09	+55:31:32.394	2	cbv+09	2130	1060	srb+15	2560	1280	srb+15
9	B2217+47	th69	22:19:48.139	3	hlk+04	+47:54:53.93	3	hlk+04	*	0	*	2520	1260	srb+15
10	B1919+21	hbp+68	19:21:44.815	2	hlk+04	+21:53:02.25	4	hlk+04	*	0	*	1860	930	srb+15
11	B1822-09	dls72	18:25:30.594	2	jbv+19	-09:35:21.2	2	jbv+19	*	0	*	1640	820	srb+15

Relevant candidate pulsar should be observable in the daylight and above the horizon, close to the zenith. So an ideal candidate would be:

B1133+16 with RA: 11:36:03.1198 Dec: +15:51:14.183

and source flux at 80MHz: 4730 +/- 2370 mJy

Here's a paper on this pulsar: It is a radio pulsar with double pulses as shown in the figure below:

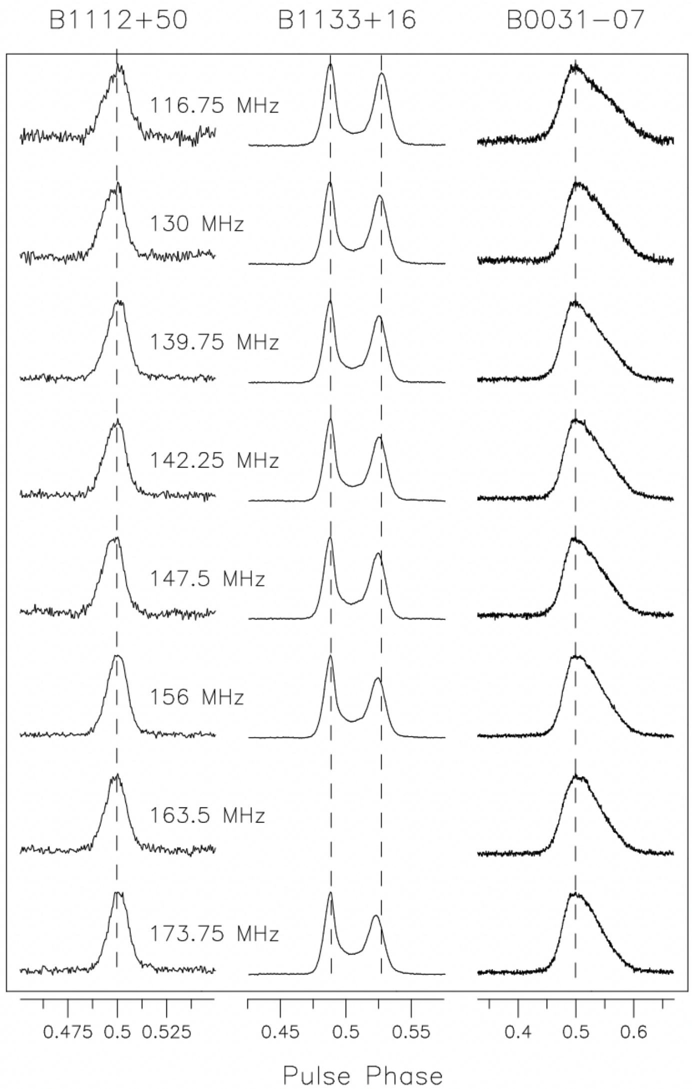

Fig. 1. Average pulse profiles of the three pulsars. The profile changes with sky frequency is clearly evident. The profile for PSR B1133+16 at 163.5 MHz is not shown because it was too corrupted by RFI. The profiles are shown at 809, 580, 460 μs time resolution for PSRs B1112+50, B1133+16 and B0031−07 respectively. All profiles are normalised by the maximum flux density in the band and are aligned at the phase of maximum intensity in each band. Profiles at 116.75 and 130 MHz have comparatively more noise because up to ~15% of pulses were removed to reject RFI.

Here's a paper on the same pulsar B1133+16 as observed using LWA.
[PULSAR OBSERVATIONS USING THE FIRST STATION OF THE LONG WAVELENGTH ARRAY AND THE LWA PULSAR DATA ARCHIVE]

This is at a much lower frequency than the previous paper.

Double pulse profile: New Features in Two Radio Pulsars: PSR 1541+ 09 and PSR 1133+ 16 (LA Nowakowski) et al model the pulse beam with two concentric emission cones.

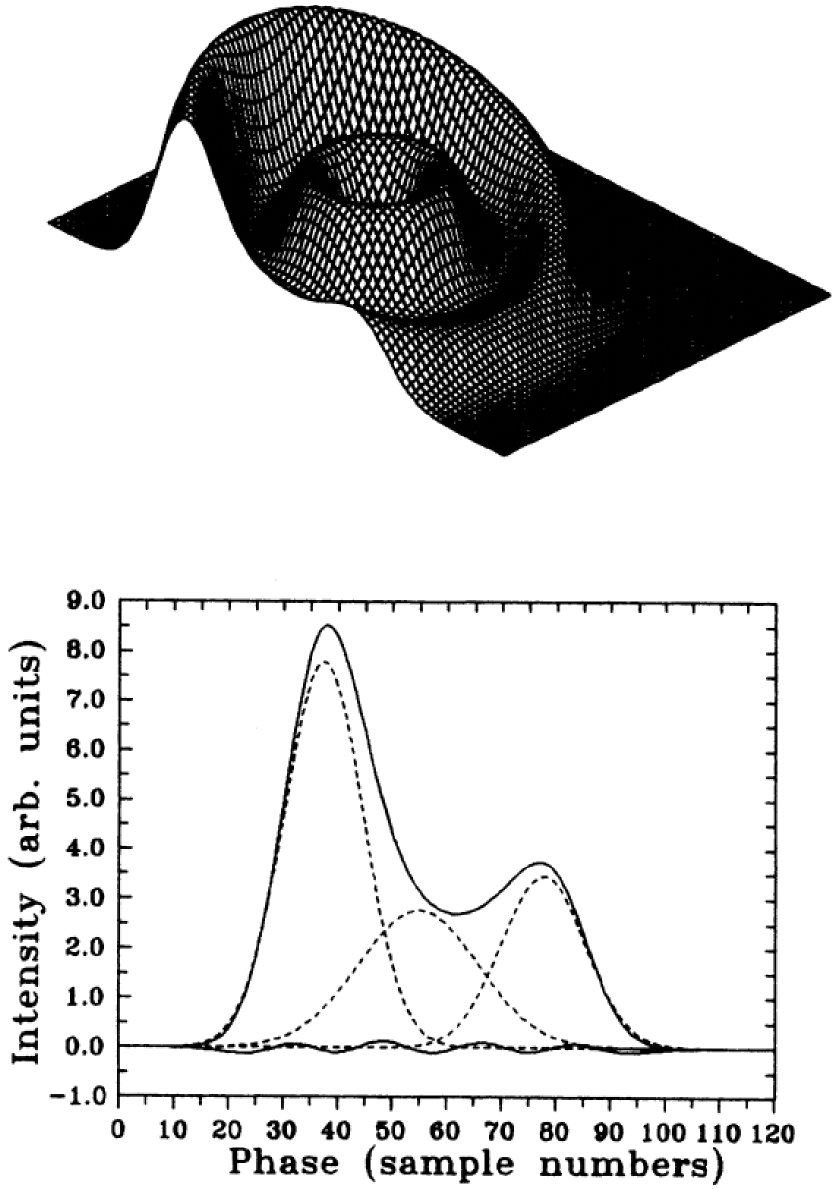

FIG. 18.—PSR 1133 + 16. One of the models of the geometry of the emitting region that we tested. Radiation comes from two concentric rings. The line of sight cuts the inner side of the outer ring and the edge of the inner ring, producing the average profile shown in the lower part of the figure. Simultaneous fitting of three Gaussians shows convincingly there are three components (the solid line around zero intensity represents residuals after three Gaussian components are subtracted from the profile). It is interesting that the profile obtained from the same configuration but *without* the inner ring produces a very similar profile that shows in an equally convincing way there are three Gaussian components as well. Thus, the inner ring is not necessary to explain the morphology of the saddle region, but this is the only configuration in which the subpulses can drift in the saddle region while the other subpulses do not drift (see Fig. 15, pulses 20–33; see also Fig. 16).